Tricritical universality in a two-dimensional spin fluid

N. B. Wilding and P. Nielaba
Institut für Physik, Johannes Gutenberg Universität, Staudinger Weg 7, D-55099 Mainz, Germany
(Received 14 August 1995)

Monte Carlo simulations are used to investigate the tricritical point properties of a two-dimensional (2D) spin fluid. Measurements of the scaling operator distributions are employed in conjunction with a finite-size scaling analysis to locate the tricritical point and determine the directions of the relevant scaling fields and their associated tricritical exponents. The scaling operator distributions and exponents are shown to match quantitatively those of the 2D Blume-Capel model, confirming that both models belong to the same universality class. Mean-field calculations of the tricritical point location are also compared with the simulation measurements.

PACS number(s): 64.70.Fx, 64.60.Fr, 05.70.Jk, 64.60.Kw

I. INTRODUCTION

For tricritical phenomena, the highest dimension in which nonclassical behavior can be observed is $d = 2$ [1]. Consequently, two-dimensional (2D) tricritical phenomena have been the subject of a large number of previous investigations, employing a wide variety of techniques, including series expansions [2], mean-field theory [3], renormalization group (RG) [4–8], transfer matrix [9–12], Monte Carlo simulations [13,14], and Monte Carlo RG methods [15–17]. To date, however, this interest has focused almost exclusively on lattice-based spin models such as the Blume-Capel model or the spin-$\frac{1}{2}$ next-nearest-neighbor Ising model. In this paper, we report a detailed simulation study of 2D tricritical behavior in an off-lattice spin fluid model.

The model we consider is a simplified representation for a liquid of two-state molecules and has been the subject of a number of previous studies in both its classical and quantum regimes [18]. In the present work, however, we shall consider only the classical limit, for which the configurational energy is given by

$$\Phi(\{\vec{r},s\}) = \sum_{i<j}^{N} -J(r_{ij})s_i s_j + \sum_{i<j}^{N} U(r_{ij}), \qquad (1.1)$$

with $s_i = \pm 1$ and where $U(r_{ij})$ is chosen to be a hard disk potential with diameter σ. The distance-dependent spin coupling parameter $J(r_{ij})$ is assigned a square well form:

$$\begin{aligned} J(r) &= J, \quad \sigma < r < 1.5\sigma, \\ J(r) &= 0, \quad \text{elsewhere.} \end{aligned} \qquad (1.2)$$

The phase diagram of this model is expected to correspond to the situation depicted schematically in Fig. 1. For high temperatures there exists a line of Ising critical points (the so-called "critical line") separating a ferromagnetic fluid phase from a paramagnetic fluid phase. The particle density varies continuously across this line. As one follows the critical line to lower temperatures, however, the size of the particle density fluctuations grows progressively. Precisely at the tricritical point, the fluctuations in both the particle density and magnetization are simultaneously divergent. Lowering the temperature still further results in a phase separation between a low density paramagnetic gas and a high density fer-

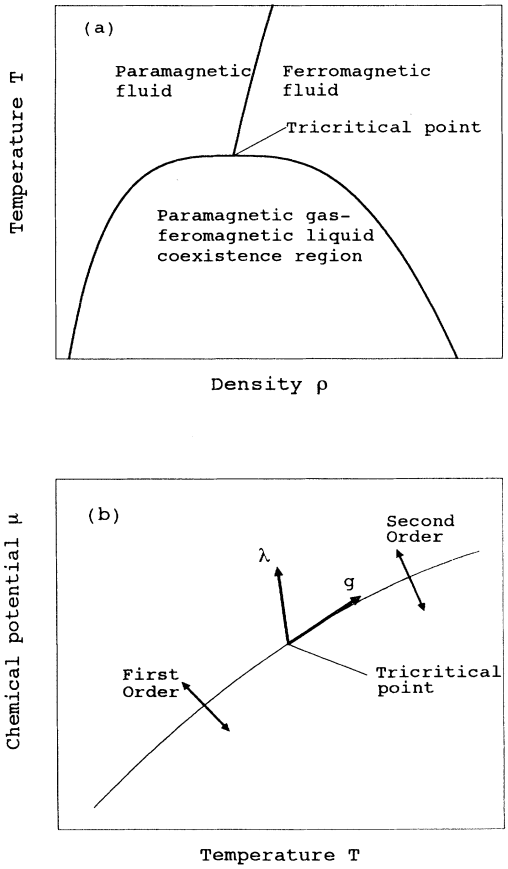

FIG. 1. (a) Schematic phase diagram of the spin fluid in the T-ρ plane. (b) Schematic phase diagram in the μ-T plane showing the directions of the relevant scaling field g and λ.

romagnetic liquid. For subtricritical temperatures, the phase transition between these two phases is first order.

Owing to the interplay between the density and magnetization fluctuations, the tricritical properties of the spin fluid system are expected to differ qualitatively from those on the critical line. General universality arguments [19] predict that for a given spatial dimensionality, fluids with short-ranged interactions should exhibit the same tricritical properties as lattice-based spin systems. However, since fluids possess a continuous translational symmetry that lattice models do not, this proposal needs be checked. Additionally, experience with "ordinary" (Ising) critical behavior in simple fluids, such as the Lennard-Jones fluid [20,21], shows that the reduced symmetry of fluids can profoundly influence certain nonuniversal aspects of the critical properties. Principal among these are the directions of the relevant scaling fields associated with the fixed point, and the distribution functions of observables, such as the particle density and energy. It is thus of interest to assess the extent of these "field-mixing" effects in the tricritical fluid and to compare it with the situation at the liquid-vapor critical point of simple fluids.

An accurate determination of the universal forms of the tricritical scaling operator distribution is also of considerable value. Such distributions are *unique* to a universality class, and hence, knowledge of their forms would be of considerable practical utility to future simulation studies of 2D tricriticality, serving as they do to simplify the computational task of locating the tricritical parameters. Moreover, as we shall see, the forms of the scaling operator distribution functions can impart important physical insight into the nature of the tricritical fluctuations.

Our paper is broadly organized as follows. In Sec. II we describe the finite-size scaling methods and other computational techniques that are employed in the study. We then proceed in Sec. III to detail the application of these techniques to Monte Carlo simulations of both the 2D spin fluid model described above and the 2D Blume-Capel model. The simulations yield accurate estimates of the location of the tricritical point for both models, as well as the universal forms of the tricritical scaling operator distributions and the directions of the relevant scaling fields. In the case of the spin fluid model, the estimates for the tricritical point parameters are compared with the results of a mean-field calculation. Finally Sec. IV details our conclusions.

II. BACKGROUND

The techniques we employ in this work have been previously developed in the context of simulation studies of Ising critical phenomena in a variety of fluid models, including a decorated lattice gas model [22,23], a lattice model for polymer mixtures [24], and both the two- and three-dimensional Lennard-Jones fluids [20,21]. In common with the strategy pursued in these previous works, we have chosen to work within the grand canonical ensemble, the use of which affords effective treatment of the particle density fluctuations that are a central feature of fluid critical behavior.

Let us assume our system to be contained in a volume L^d, with $d = 2$ in the simulations to be described later. The grand partition function is given by

$$\mathcal{Z}_L = \sum_{N=0}^{\infty} \sum_{\{s_i\}} \prod_{i=1}^{N} \left\{ \int d\vec{r}_i \right\} \times \exp\left\{ -\beta \left[\Phi(\{\vec{r}, s\}) + \mu N + H \sum_{j=1}^{N} s_j \right] \right\}, \quad (2.1)$$

where N is the particle number, $\beta = (k_B T)^{-1}$ is the inverse temperature, μ is the chemical potential, and H is the uniform applied magnetic field.

The observables of chief concern to the present study are the (reduced) particle density

$$\rho = L^{-d} N \sigma^d, \quad (2.2)$$

the configurational energy density (which we express in units of J)

$$u = L^{-d} J^{-1} \Phi(\{\vec{r}, s\}), \quad (2.3)$$

and the magnetization.

$$m = L^{-d} \sum_i s_i. \quad (2.4)$$

The coarse-grained behavior of the system in the vicinity of the tricritical point is controlled by three relevant scaling fields [1,25,26], which we denote g, λ, and h'. In general these scaling fields are each expected to comprise linear combinations of the three thermodynamic fields T, μ, and H [27,12]. For the spin fluid model considered in this paper, however, the configurational energy is invariant with respect to sign reversal of the spin degrees of freedom. This special symmetry implies that the tricritical point lies in the symmetry plane $H = 0$, and that the scaling field h' coincides with the magnetic field H, being orthogonal to the μ-T plane containing the other two scaling fields, g and λ. Thus we can write

$$h' = H - H_t, \quad (2.5a)$$

$$\lambda = (\mu - \mu_t) + r(T - T_t), \quad (2.5b)$$

$$g = T - T_t + s(\mu - \mu_t), \quad (2.5c)$$

where the subscript t signifies tricritical values and the parameters s and r are system-specific "field mixing" parameters that control the directions of the scaling fields in the μ-T plane. The scaling fields g and λ are depicted schematically in Fig. 1(b). One sees that g is tangent to the coexistence curve at the tricritical point [25], so that the field mixing parameter r may be identified simply as the limiting tricritical gradient of the coexistence curve. The scaling field λ, on the other hand, is permitted to take a general direction in the μ-T plane, which does not necessarily have to coincide with any special direction of the phase diagram [27].

Conjugate to each of the scaling fields are scaling op-

erators, defined by the requirements

$$\langle \mathcal{M} \rangle \equiv L^{-d} \partial \ln \mathcal{Z}_L / \partial h', \tag{2.6a}$$

$$\langle \mathcal{D} \rangle \equiv L^{-d} \partial \ln \mathcal{Z}_L / \partial \lambda, \tag{2.6b}$$

$$\langle \mathcal{E} \rangle \equiv L^{-d} \partial \ln \mathcal{Z}_L / \partial g, \tag{2.6c}$$

from which it follows [utilizing Eqs. (2.1) and (2.5a)–(2.5c)], that

$$\mathcal{M} = m, \tag{2.7a}$$

$$\mathcal{D} = \frac{1}{1 - sr}[\rho - su], \tag{2.7b}$$

$$\mathcal{E} = \frac{1}{1 - sr}[u - r\rho]. \tag{2.7c}$$

Drawing on our experience with ordinary critical phenomena in simple fluids [20] we make the following finite-size scaling ansatz [28] for the limiting (large L) near-tricritical distribution of $p_L(\rho, u, m)$:

$$p_L(\rho, u, m) \simeq \frac{1}{1 - sr} \tilde{p}_L(a_1^{-1} L^{d-y_1} \mathcal{M}, a_2^{-1} L^{d-y_2} \mathcal{D}, a_3^{-1} L^{d-y_3} \mathcal{E}, a_1 L^{y_1} h', a_2 L^{y_2} \lambda, a_3 L^{y_3} g), \tag{2.8}$$

where $\tilde{p}_L$ is a universal scaling function, the a_i are nonuniversal metric factors, and the y_i are the standard tricritical eigenvalue exponents [29]. Precisely at the tricritical point, the tricritical scaling fields vanish identically and the last three arguments of Eq. (2.8) can be simply dropped, yielding

$$p_L(\rho, u, m) \simeq \frac{1}{1 - sr} \tilde{p}^{\star}_L(a_1^{-1} L^{d-y_1} \mathcal{M}, a_2^{-1} L^{d-y_2} \mathcal{D}, a_3^{-1} L^{d-y_3} \mathcal{E}), \tag{2.9}$$

where $\tilde{p}^{\star}_L$ is a universal and scale invariant function characterizing the tricritical fixed point.

In what follows we shall explicitly test the proposed universality of Eq. (2.9) for the case of the spin fluid model, by obtaining the form of $\tilde{p}^{\star}_L$ and comparing it with that for the tricritical 2D Blume-Capel model.

III. RESULTS

A. Computational aspects

The Monte Carlo simulations of the spin fluid model were performed using a Metropolis algorithm within the grand canonical ensemble. Particle insertions and deletions were carried out using the prescription of Adams [30,31]. When attempting particle insertions the spin of the candidate particle was randomly assigned the value $+1$ or -1 with equal probability. Spin flip attempts were performed at the same frequency as insertion-deletion attempts.

In order to facilitate efficient computation of interparticle interactions, the periodic simulation space of volume L^2 was partitioned into l^2 square cells each of side 1.5σ, corresponding to the interaction range of the interparticle potential [cf. Eq. (1.1)]. This strategy ensures that interactions emanating from particles in a given cell extend at most to particles in the eight neighboring cells. We chose to study three system sizes corresponding to $l = 12, 16$, and 20, containing, at coexistence, average particle numbers of $\langle N \rangle = 120$, 210, and 330, respectively. For the $l = 12, 16$, and 20 system sizes, equilibration periods of 10^5 Monte Carlo transfer attempts *per cell* (MCS) were utilized, while for the $l = 16$ and $l = 20$ system sizes up to 2×10^6 MCS were employed. Sampling frequencies ranged from 25 MCS for the $l = 12$ system to 100 MCS for the $l = 20$ system. Production runs amounted to 1×10^7 MCS for the $l = 12$ and up to 5×10^7 MCS for the $l = 20$ system size. At coexistence the average acceptance rate for particle transfers was approximately 16%, while for spin flip attempts the acceptance rate was approximately 5%.

During the production runs, the joint probability distribution $p_L(\rho, u, m)$ was obtained in the form of a histogram. In order to increase computational efficiency, the histogram extrapolation technique [32] was employed. Use of this technique permits histograms obtained at one set of model parameters to be reweighted to yield estimates appropriate to another set of model parameters. The method is particularly effective close to a critical point where, owing to the large fluctuations, a single simulation permits extrapolation over the entire critical region.

As an aid to locating the tricritical point, the cumulant intersection method was employed [33]. The fourth order cumulant ratio U_L is a quantity that characterizes the form of a distribution [34]. It is defined in terms of the fourth and second moments of a given distribution,

$$U_L = 1 - \frac{\langle m^4 \rangle}{3 \langle m^2 \rangle^2} . \tag{3.1}$$

The tricritical scale invariance of the distributions $p_L(\mathcal{D}), p_L(\mathcal{M})$, and $p_L(\mathcal{E})$ [as expressed by Eq. (2.9)] implies that at the tricritical point (and modulo corrections to scaling), the cumulant values for all system sizes should be equal. The tricritical parameters can thus be found by measuring U_L for a number of temperatures and system sizes along the first order line, according to the prescription given below. Precisely at the tricritical temperature the curves of U_L corresponding to the various system sizes are expected to intersect one another at a single common point.

B. The 2D Blume-Capel model

In seeking to confirm the proposed universality linking the tricritical point of the 2D spin fluid model to those of 2D lattice models, it is first necessary to determine the tricritical operator distribution functions for a simple lattice model. To this end we have also performed a simulation study of the Blume-Capel model on a periodic square lattice, the Hamiltonian of which is given by

$$\mathcal{H} = -J \sum_{\langle i,j \rangle} s_i s_j + D \sum_i s_i^2 + H \sum_i s_i, \qquad (3.2)$$

with $s_i = -1, 0, 1$. Here H is a uniform magnetic field and D is the so-called "crystal field." As with the 2D spin fluid model, the symmetry of the configurational energy under spin sign reversal implies that the tricritical point lies in the symmetry plane $H = 0$.

Previous MCRG [15,16] investigations place the tricritical point of the 2D Blume-Capel model at $k_B T_t/J = 0.609(3), D_t = 1.965(15)$, while a more recent transfer matrix study [9] gives $k_B T_t/J = 0.610(5), D_t = 1.965(5)$. Using these estimates as an initial guide, we performed extensive Monte Carlo simulations of the model using a vectorized Metropolis algorithm on a Cray-YMP. Four system sizes of linear extent $L = 12, 20, 32, 40$ were studied, and following equilibration, runs ranging from 5×10^6 Monte Carlo sweeps (MCS) for the L=12 system, to 2×10^7 MCS for the L=40 system were performed. The quantities measured in the course of these runs were

$$\rho' = \sum s_i^2, \qquad (3.3a)$$

$$u = -J \sum_{\langle i,j \rangle} s_i s_j, \qquad (3.3b)$$

$$m = \sum s_i. \qquad (3.3c)$$

Here we note that $\rho' = \sum s_i^2$ plays the same role as the density in the spin fluid model, being discontinuous across the first order line but continuous on the critical line. This fact is most clearly evident in the lattice gas representation of the Blume-Capel model, where the crystal field D appears as a chemical potential [35].

During the simulations, the joint distribution $p_L(\rho', u, m)$ was collected in the form of a histogram. To determine the locus of the first order line (and hence locate the tricritical point in which it formally terminates), the coexistence symmetry criterion for the operator distribution $p_L(\mathcal{D})$ was utilized. This criterion is the analog for asymmetric first order transitions, of the order-parameter distribution symmetry condition applicable to symmetric first order transitions such as that of the subcritical simple Ising model [23]. For a given temperature T, the first order transition point can thus be located by tuning the crystal field D and the value of the field mixing parameter s, within the histogram reweighting scheme, until the operator distribution $p_L(\mathcal{D})$ is symmetric in $\mathcal{D} - \langle \mathcal{D} \rangle$.

The first order line and its finite-size analytical extension [20] was determined in this way for temperatures in the range $k_B T/J = 0.59$–0.625, and for each of the four system sizes. The corresponding values of the cumulant ratio $U_L^{\mathcal{D}}$ *along* this coexistence line are presented in Fig. 2 as a function of the temperature. To within numerical uncertainties the cumulant values for each system size intersect at a common temperature, which we estimate as $k_B T_t/J = 0.608(1)$. The corresponding estimate for the tricritical field is $D_t = 1.9665(3)$. Clearly these values are in excellent agreement with the aforementioned estimates of previous studies. In the following subsection we compare the measured forms of the tricritical operator distributions $p_L(\mathcal{M})$, $p_L(\mathcal{D})$, and $p_L(\mathcal{E})$ of the 2D Blume-Capel, with those of the 2D spin fluid model.

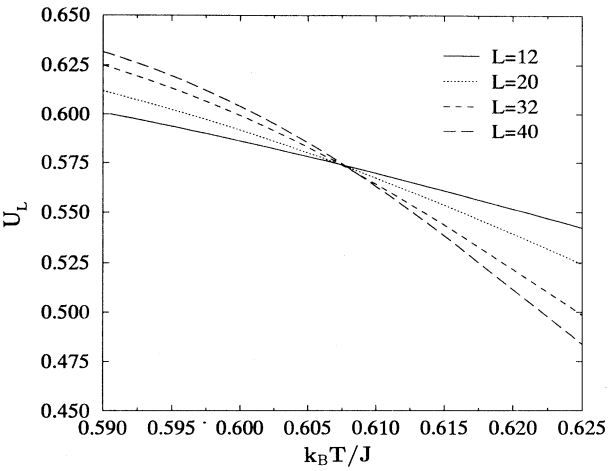

FIG. 2. Measured cumulant ratio $U_L^{\mathcal{D}}$ for the 2D Blume-Capel model along the first order line and its analytic extension, determined according to the procedure described in the text.

C. The spin fluid model

The procedure for locating the tricritical point of the 2D spin fluid model followed the same pattern as that for the 2D Blume-Capel model described above, except that in the present case no prior estimates for the tricritical point were available. It was thus necessary to search for the approximate location of the tricritical point by performing a number of short runs in which a temperature was chosen and the chemical potential tuned. Observations of the behavior of the density from these short runs suggested that the tricritical point lay close to the parameters $k_B T/J = 0.58$, $\beta\mu = -1.915$.

Having obtained an approximate estimate of the location of the tricritical point, long runs were carried out for each of the three system sizes $l = 12, 16, 20$. As with the Blume-Capel model, the coexistence symmetry condition was then applied to the operator distribution $p_L(\mathcal{D})$ in conjunction with the histogram reweighting scheme, in order to determine the first order line and its analytic extension in the μ-T plane. The locus of this line is shown in Fig. 3, while the measured values

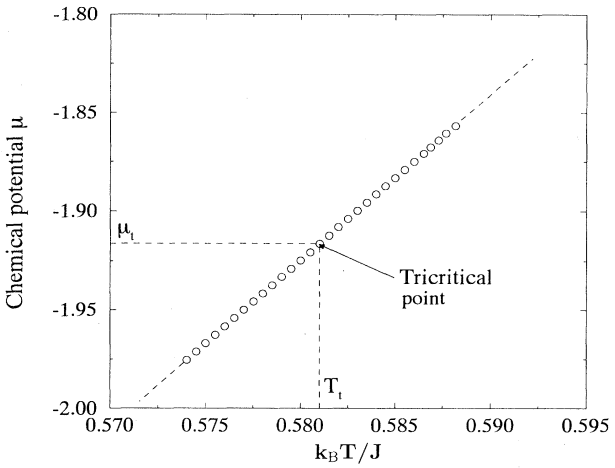

FIG. 3. Line of first order transitions and its finite-size analytical extension in the μ-T plane, obtained according to the procedure described in the text.

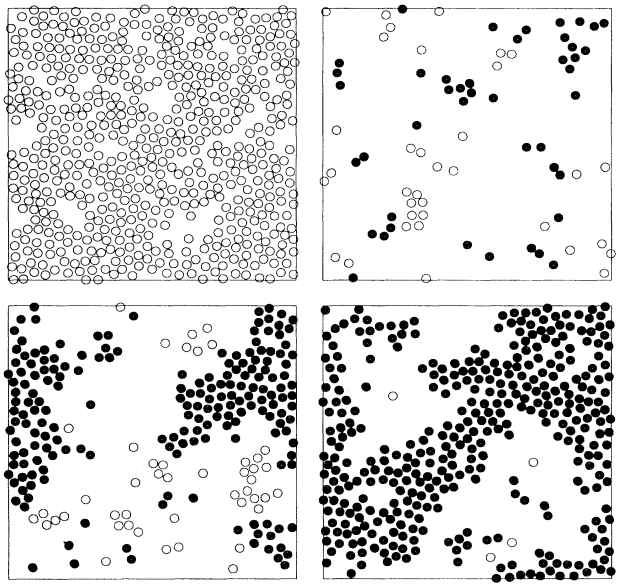

FIG. 5. Typical particle-spin configurations of the $l = 20$ spin fluid near tricriticality. Spins values of $+1$ are denoted by filled circles, and spin values -1 by unfilled circles.

of $U_L^{\mathcal{D}}$ along this coexistence line are shown in Fig. 4 for the three system sizes $l = 12, 16, 20$. Clearly the curves of Fig. 4 have a single well-defined intersection point, from which we estimate the tricritical temperature as being $k_B T_t/J = 0.581(1)$. The associated estimate for the chemical potential is $\beta\mu_t = -1.916(2)$. Typical near-tricritical configurations for the $l = 20$ system are shown in Fig. 5.

In Fig. 6 we present the forms of the operator distributions $p_L(\mathcal{M})$, $p_L(\mathcal{D})$, and $p_L(\mathcal{E})$ corresponding to the designated values of the tricritical parameters. The value of the field mixing parameter r implicit in the definition of $\mathcal{E}$ was assigned the value $r = -2.82$, as obtained from the measured gradient of the phase boundary in the μ-T plane at the tricritical point. The value of the field mixing parameter s was assigned, as previously described, so that $p_L(\mathcal{D})$ satisfied the symmetry condition. However, the resulting estimates of s were found to exhibit a systematic finite-size dependence. This effect has also been previously noted (albeit with much reduced magnitude) in a recent study of critical phenomena in the Lennard-Jones fluid, and is traceable to the finite-size dependence of the average critical energy [23,20]. For the three system sizes, $l = 12, 16, 20$, we found $s = -0.031, -0.020, -0.013$, respectively. Interestingly, these values are about an order of magnitude smaller than those measured at the critical point of the 2D and 3D Lennard-Jones fluid, a finding which we discuss further in Sec. IV. This smallness implies that the scaling field λ almost coincides with the μ axis of the phase diagram.

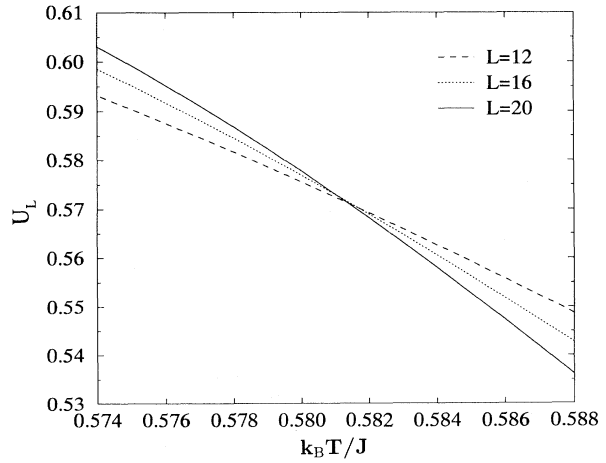

FIG. 4. Measured cumulant ratio $U_L^{\mathcal{D}}$ for the 2D spin fluid model along the first order line and its analytic extension determined according to the procedure described in the text.

Also included in Fig. 6 are the measured tricritical operator distributions for the 2D Blume-Capel model. In accordance with convention, all the operator distributions have been scaled to unit norm and variance. Clearly in each instance and for each system size, the operator distributions collapse extremely well onto one another, as well as onto those of the tricritical Blume-Capel model.

The measured scaling operator distributions also serve to furnish estimates of the eigenvalue exponents y_1, y_2, and y_3, characterizing the three relevant scaling fields. These exponents are accessible via the respective finite-size scaling behavior of the tricritical distributions of $p_L(\mathcal{M})$, $p_L(\mathcal{D})$, and $p_L(\mathcal{E})$. Specifically, consideration of the scaling form (2.9) shows that the typical size of the fluctuations in a given operator $\mathcal{O}$ vary with system size, such as $\delta\mathcal{O} \sim L^{-(d-y_i)}$. A comparison of the standard deviation of a given operator distributions

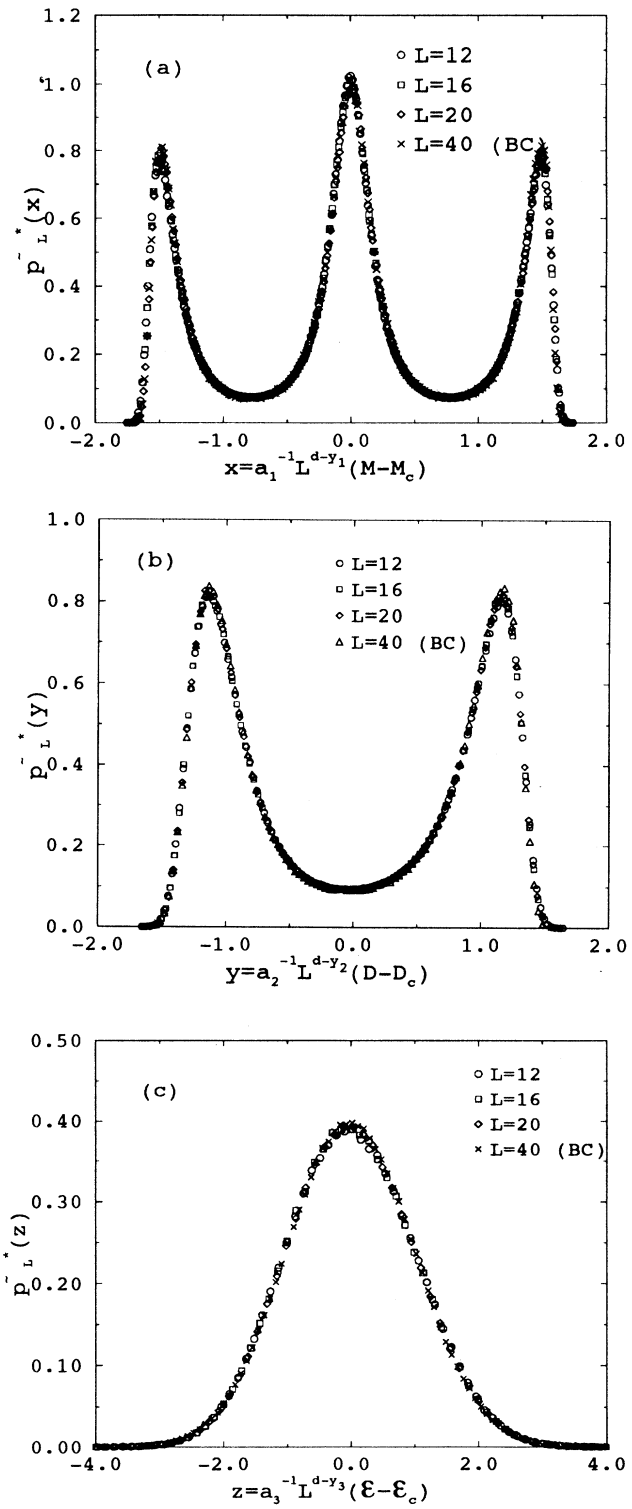

FIG. 6. Scaling operator distributions for the 2D spin fluid at the designated tricritical parameters for each of the three system sizes $l = 12, 16, 20$. (a) $\tilde{p}_L^*(\mathcal{M})$, (b), $\tilde{p}_L^*(\mathcal{D})$, (c) $\tilde{p}_L^*(\mathcal{E})$. Also shown for comparison are the corresponding distributions measured for the tricritical $L = 40$ 2D Blume-Capel model. All distributions are expressed in terms of the scaling variable $a_i^{-1}L^{d-y_i}(\mathcal{O} - \mathcal{O}_c)$ and are scaled to unit norm and variance. Statistical errors do not exceed the symbol sizes.

as a function of system size thus affords estimates of the appropriate exponents. From the measured variance of the spin fluid operator distributions, we find $y_1 = 1.93(1)$, $y_2 = 1.80(1)$, $y_3 = 1.03(7)$. As far as y_1 and y_2 are concerned, these estimates are in excellent agreement with exact conjectures $y_1 = 77/40$, $y_2 = 9/5$ [36–38]. The situation regarding the eigenvalue exponent y_3, on the other hand, is not so satisfactory, there being a sizable discrepancy with the exact value of $y_3 = 4/5$. This discrepancy stems, we believe, from two sources. First, since the operator distribution $p_L(\mathcal{E})$ is highly sensitive with respect to the designation of the value of the field mixing parameter r implicit in the definition of $\mathcal{E}$, small uncertainties in the estimate of r can lead to significantly larger errors in the measured variance of $p_L(\mathcal{E})$. A similar effect was also previously observed at the liquid-vapor critical point of the Lennard-Jones fluid [21]. Second, and as we discuss in Sec. IV, the near Gaussian character of $p_L(\mathcal{E})$ signifies the absence of strong fluctuations in the $\mathcal{E}$, in which case it is questionable whether a finite-size scaling analysis can be reliable when applied to $p_L(\mathcal{E})$ at all.

In view of this problem we have adopted a rather different approach for measuring y_3 based on the scaling properties of $U_L^{\mathcal{D}}$, a quantity that does show strong fluctuations and that is also insensitive to the designation of the field mixing parameter r. It can be shown [33] that the maximum slope of the cumulant ratio $\frac{dU_L}{dT}$ near T_c varies with system size like L^{y_3}. Using the histogram extrapolation technique, we have obtained the temperature dependence of this slope for the spin fluid model. The results yield the estimate $y_3 = 0.83(5)$, which agrees to within error with the exact conjecture.

Turning now to the observables m, ρ, and u, we plot in Fig. 7 the measured distributions of these quantities at the assigned tricritical parameters. Here we note that as is the case with ordinary critical phenomena in the Lennard-Jones fluid [21], the energy distribution $p_L(u)$ differs qualitatively in form from the operator distribution $p_L(\mathcal{E})$. This finding, the origin of which is explained in detail in Ref. [23], reflects the coupling of the tricritical energy fluctuations to the density, the latter of which are stronger and thus dominate for large L. The influence of this coupling is also discernible as a small asymmetry in the tricritical density distribution. For the average tricritical density we find $\rho_t = 0.374(1)$, while for the average tricritical energy density we find $u_t = 0.778(2)$. The average magnetization is of course strictly zero on symmetry grounds.

Finally in this subsection, Table I summarizes the measured values of the fourth order cumulant ratios $U_L^{\mathcal{O}}$ for each of the three scaling operator distributions at the assigned values of the tricritical parameters.

TABLE I. Fourth order cumulant ratio for the tricritical fixed point operator distributions.

$U_L^{\mathcal{M}}$	0.348(3)
$U_L^{\mathcal{D}}$	0.574(2)
$U_L^{\mathcal{E}}$	0.003(3)

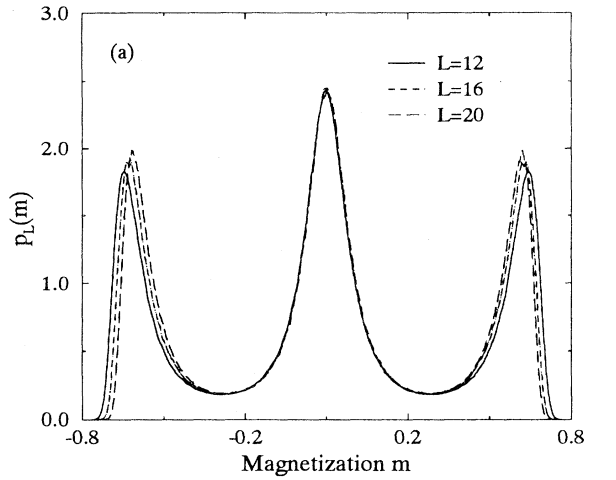

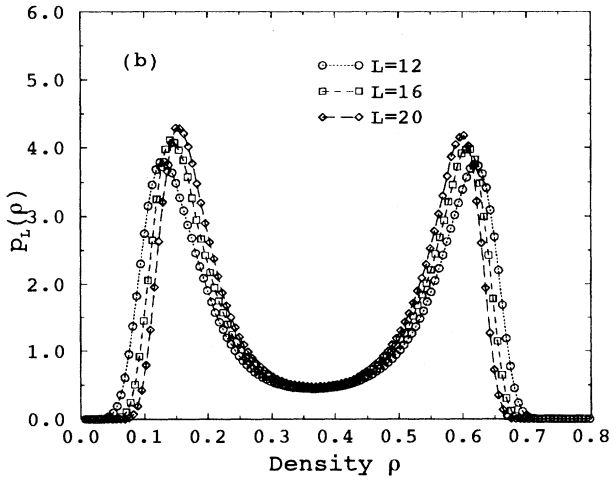

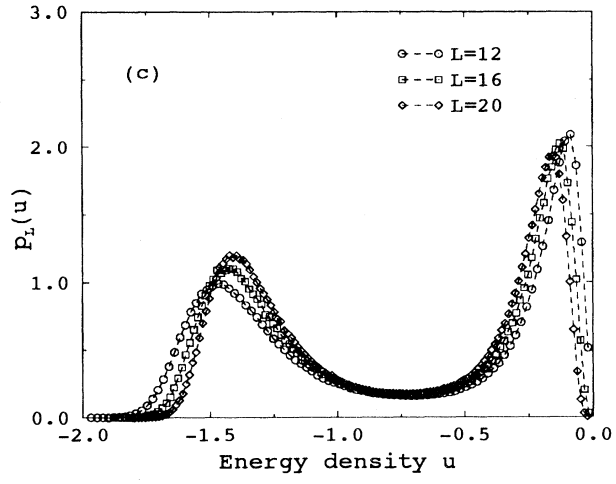

FIG. 7. Measured tricritical point forms of (a) the magnetization distribution $p_L(m)$ (the data points have been suppressed for clarity); (b) the density distribution $p_L(\rho)$; (c) the energy density distribution $p_L(u)$.

1. Mean-field calculations

In this section we describe a simple mean-field calculation of the tricritical parameters of the 2D spin fluid. Let $p(\rho,\mu;h)$ denote the pressure in the system for a given chemical potential μ and volume V in the thermodynamic limit, where the equilibrium density ρ is given by the ratio of the average number of particles $\langle N\rangle$ and the volume V, $\rho = \lim_{V\to\infty}(\langle N\rangle/V)$. Then

$$p(\rho,\mu;h) = \min_{\rho'}\left[-f(\rho';h) + \mu\rho'\right], \tag{3.4}$$

where $f(\rho';h)$ is the free energy per volume,

$$f(\rho';h) = \lim_{V\to\infty}\frac{-1}{\beta V}\ln \mathrm{tr}\{\exp[-\beta H^N(h)]\}\ . \tag{3.5}$$

In the mean-field approximation we assume an interaction between a spin s_1 and an effective field $(q/N)\sum_{i>1}s_i = qm$, where q is the effective coordination number and the N-particle Hamiltonian is written as

$$H^N_{MF} = \sum_{(i<j)} U(r_{ij}) - \sum_{i=1}^{N}\left[qm(h)+h\right]s_i \tag{3.6}$$

and the mean-field free energy f_{MF} is

$$f_{MF}(\rho';h) = \lim_{V\to\infty}\frac{-1}{\beta V}\ln \mathrm{tr}\{\exp[-\beta H^N_{MF}(h)]\}, \tag{3.7}$$

$$f_{MF}(\rho';h) = f_{cl}(\rho') + \min_m\left[\frac{q\rho' m^2}{2} - \frac{\rho'}{\beta}\ln 2\cosh\left[\beta(qm+h)\right]\right]\ . \tag{3.8}$$

$f_{cl}(\rho')$ is the free energy of a classical system with Hamiltonian $H_{cl} = \sum_{(i<j)}U(r_{ij})$ and the second term on the right-hand side of Eq. (3.8) reaches its minimum at

$$m(h) = \tanh\{\beta[qm(h)+h]\}. \tag{3.9}$$

Since the coordination number q in the fluid is not fixed we approximate the effective field on one particle by

$$qm = m\rho'\int d^2r J(r)g(r), \tag{3.10}$$

where the fluid correlation function $g(r)$ is taken from the Percus-Yevick solution for hard discs, which can be found numerically.

Two phase coexistence between a gas phase at density ρ_g and a liquid phase at density ρ_l is given by equal pressure in the two phases,

$$p(\rho_g,\mu;h) = p(\rho_l,\mu;h)\ . \tag{3.11}$$

This condition determines the mean-field chemical potential μ_{MF} for phase coexistence via Eq. (3.4). Implementing this criterion numerically, we find $T_t^{MF} = 1.006$ $\beta\mu_t^{MF} = -1.319$. Clearly this estimate for T_t seri-

ously overestimates the measured tricritical temperature ($T_t = 0.581$) showing that mean-field calculations of this type cannot be relied upon to provide accurate tricritical data, at least for 2D systems.

IV. CONCLUSIONS

In summary we have demonstrated that the tricritical ordering operator distributions of the 2D spin fluid can be mapped into excellent correspondence with those of the 2D Blume-Capel model. The existence of such a mapping represents perhaps the most stringent test of universality. There can thus be little doubt that despite their very different microscopic character, the two systems do indeed share a common fixed point.

With regard to the scaling operator distribution themselves, we note that the form of $p_L^\star(\mathcal{E})$ is (to within the precision of our measurements) essentially Gaussian, as evidenced by the very small value of the cumulant ratio $U_L^{\mathcal{E}} = 0.003(3)$. This Gaussian behavior implies that the tricritical fluctuations in $\mathcal{E}$ are extremely weak and is thus a consequence of the central limit theorem. This weakness is further manifest in the very small measured values of the field mixing parameter s, as well as in the near absence of asymmetry in the tricritical density distributions, a situation that contrasts markedly with that of the 2D and 3D Lennard-Jones fluids, where much stronger field mixing effects are observed in the density distribution [21].

Finally, the tricritical form of $\tilde{p}_L^\star(\mathcal{M})$ merits special comment. We note that the *three-peaked* form of this distribution differs radically from the universal magnetization distribution of the critical Ising model, which is strongly *double-peaked* in two dimensions [33,39]. The existence of a three-peaked structure for tricritical phenomena reflects the additional coupling that arises between the magnetization and the density fluctuations. Specifically, the central peak corresponds to fluctuation to small density, which are concomitant with an overall reduction in the magnitude of the magnetization (cf. Fig. 5). Were one, however, to depart from the tricritical point along the critical line, these density fluctuations would gradually die out and a crossover to a magnetization distribution having the double-peaked Ising form would be expected. In future work we intend to investigate the nature of this crossover in detail.

ACKNOWLEDGMENTS

A generous allocation of Cray-YMP computer time at the RHRK, Universität Kaiserslautern and HLRZ, Jülich is gratefully acknowledged. The authors have benefited from helpful discussions with K. Binder, B. Dünweg, K. K. Mon, and M. Müller. N.B.W. acknowledges the financial support of the Commission of the European Community (ERB CHRX CT-930 351). P.N. thanks the DFG for financial support (Heisenberg foundation)

[1] For a general review of tricritical phenomena, see I.D. Lawrie and S. Sarbach, in *Phase Transitions and Critical Phenomena*, edited by C. Domb and J.L. Lebowitz (Academic, London, 1984), Vol. 8.
[2] D.M. Saul, M.W. Ortis, and D. Stauffer, Phys. Rev. B **9**, 4964 (1974).
[3] D. Furman, S. Dattagupta, and R.B. Griffiths, Phys. Rev. B **15**, 441 (1977).
[4] S.M. de Oliveira, P.M.C. de Oliveira, and F.C. de Sá Barreto, J. Stat. Phys. **78**, 1619 (1995).
[5] A. Bakchich, A.N. Benyoussef, and M. Touzani, Physica A **186**, 524 (1992).
[6] T.W. Burkhardt and H.J.F. Knops, Phys. Rev. B **15**, 1602 (1977).
[7] A.N. Berker and H.J.F. Knops, Phys. Rev. B **15**, 1602 (1977).
[8] J.M. Yeomans and M.E. Fisher, Phys. Rev. B **24**, 2825 (1981).
[9] P.D. Beale, Phys. Rev. B **33**, 1717 (1986).
[10] H.J. Herrmann, Phys. Lett. **100A**, 256 (1984).
[11] P.A. Rikvold, W. Kinzel, J.D. Gunton, and K. Kaski, Phys. Rev. B **28**, 2686 (1983).
[12] F.C. Alcaraz, J.R. Drugowich de Felicio, R. Köberle, and J.F. Stilck, Phys. Rev. B **32**, 7469 (1985).
[13] K.L. Ayat and C.M. Care, J. Magn. Magn. Mater. **127**, L20 (1993).
[14] J.D. Kimel, S. Black, P. Carter and Y.-L. Wang, Phys. Rev. B **35**, 3347 (1987).
[15] D.P. Landau and R.H. Swendsen, Phys. Rev. B **33**, 7700 (1986).
[16] D.P. Landau and R.H. Swendsen, Phys. Rev. Lett. **46**, 1437 (1981).
[17] Y. Honda, Phys. Lett. A **184**, 74 (1993).
[18] See, e.g., R.M. Stratt, J. Chem. Phys. **80**, 5764 (1988); D. Marx, P. Nielaba, and K. Binder, Phys. Rev. B **47**, 7788 (1993); P. de Smedt, P. Nielaba, J.L. Lebowitz, J. Talbot, and L. Dooms, Phys. Rev. A **38**, 1381 (1988), and references therein.
[19] L.P. Kadanoff, in *Phase Transitions and Critical Phenomena*, edited by C. Domb and M.S. Green (Academic, New York, 1976), Vol. 5A, pp. 1–34.
[20] N.B. Wilding and A.D. Bruce, J. Phys. Condens. Matter **4**, 3087 (1992); A.D. Bruce and N.B. Wilding, Phys. Rev. Lett. **68**, 193 (1992).
[21] N.B. Wilding, Phys. Rev. E **52**, 602 (1995).
[22] N.B. Wilding, Z. Phys. B **93**, 119 (1993).
[23] N.B. Wilding and M. Müller, J. Chem. Phys. **102**, 2562 (1995).
[24] M. Müller and N.B. Wilding, Phys. Rev. E **51**, 2079 (1995).
[25] R.B. Griffiths, Phys. Rev. B **7**, 545 (1973).
[26] F.J. Wegner, Phys. Rev. B **5**, 4529 (1972).

[27] J.J. Rehr and N.D. Mermin, Phys. Rev. A **8**, 472 (1973).
[28] For a review of finite-size scaling methods, see *Finite Size Scaling and Numerical Simulation of Statistical Systems*, edited by V. Privman (World Scientific, Singapore, 1990).
[29] It should be noted that for large values of the argument $a_1 L^{y_1} g$ a crossover occurs to standard Ising critical behavior on the critical line. Such crossover phenomena can also be explicitly incorporated within the finite-size scaling framework, see, e.g., K. Binder and H.-P. Deutsch, Europhys. Lett. **18**, 667 (1992).
[30] D.J. Adams, Mol. Phys. **29**, 307 (1975).
[31] M.P. Allen and D.J. Tildesley, *Computer Simulation of Liquids* (Oxford University Press, Oxford, 1987).
[32] A.M. Ferrenberg and R.H. Swendsen, Phys. Rev. Lett. **61**, 2635 (1988); **63**, 1195 (1989).
[33] K. Binder, Z. Phys. B **43**, 119 (1981).
[34] H. Cramér, *Mathematical Methods of Statistics* (Princeton University Press, Princeton, NJ, 1946).
[35] J. Lajzerowicz amd J. Sivardière, Phys. Rev. B **11**, 2079 (1975).
[36] B. Neinhuis, A.N. Berker, E.K. Reidel, and M. Schick, Phys. Rev. Lett. **43**, 737 (1979).
[37] M.P.M. den Nijs, J. Phys. A **12**, 1857 (1979).
[38] R.B. Pearson, Phys. Rev. B **22**, 2579 (1980).
[39] D. Nicolaides and A.D. Bruce, J. Phys. A **21**, 233 (1988).